Intravenous and Intra-Arterial Oxygen-15-Labeled Water and Fluorine-18-Labeled Fluorouracil in Patients with Liver Metastases from Colorectal Carcinoma

Antonia Dimitrakopoulou-Strauss, Ludwig G. Strauss, Peter Schlag, Peter Hohenberger, Gisela Irngartinger, Franz Oberdorfer, Josef Doll and Gerhard van Kaick

Departments of Oncological Diagnostics and Therapy, Biophysics and Medical Radiation Physics and Radiochemistry and Radiopharmacology, German Cancer Research Center, Heidelberg; and Department of Surgery and Surgical Oncology, Virchow-Klinikum, Robert-Rössle-Klinik, Berlin, Germany

Intra-arterial chemotherapy can potentially increase drug delivery at the tumor sites and has therefore been used for the therapy of metastatic colorectal cancer. **Methods:** Dynamic PET and [^{18}F]fluorouracil (^{18}F-FU) were used in patients with liver metastases from colorectal cancer to examine the pharmacokinetics of the drug up to 120 min after intravenous and intra-arterial injection of the same dose of fluorouracil (FU). All patients included in the study (n = 15) had surgically implanted catheters in the gastroduodenal artery. Dynamic PET studies (up to 5 min) with ^{15}O-labeled water were performed for the evaluation of the access to the lesions immediately before the ^{18}F-FU study using both administration routes. The final evaluation included 24 metastases, obtained from 15 patients. **Results:** Of 24 lesions, 21 (87.5%) showed an improved access using the intra-arterial approach, and 20 (83.3%) demonstrated a better FU influx after intra-arterial ^{18}F-FU infusion. Metastases reached the highest ^{18}F-FU concentrations after intra-arterial administration, with a maximum standardized uptake values of 18.75 for the FU influx and of 5.03 for FU trapping. Of 24 metastases, eight (33.3%) demonstrated enhanced FU trapping after the intra-arterial administration. Cluster analysis revealed a group of metastases (n = 6) with a nonperfusion-dependent FU transport using the intravenous application. Of these six lesions, five (83.3%) did not show any enhancement of the ^{18}F-FU trapping after intra-arterial application. The data gave evidence for at least one different, energy-dependent transport system, which can be saturated even after intravenous administration of the drug. **Conclusion:** The data show that the main limiting factor for a therapy response is the very high and rapid elimination of the cytostatic agent out of the tumor cells. Furthermore, it was not possible to predict the pharmacokinetics of FU after intra-arterial application using an intravenous PET study. It may be possible, using intravenous PET double-tracer studies, to identify metastases having a nonperfusion-dependent transport system and exclude them from an intra-arterial treatment protocol.

Key Words: PET; fluorine-18-fluorouracil; oxygen-15-water; liver metastases

J Nucl Med 1998; 39:465–473

Although PET has been increasingly used to obtain quantitative data about the metabolism of malignant lesions, little is known about the use of radiolabeled drugs. PET studies with [^{18}F]fluorodeoxyglucose (FDG) help to improve tumor staging and therapy management if multiple follow-up studies are performed (*1,2*). In contrast to FDG, radiolabeled cytostatic drugs provide a direct measurement of the distribution of a chemotherapeutic agent in the target area. Therefore, chemotherapy management can be optimized either using metabolic studies with FDG or studies with radiolabeled cytostatic agents (*2,3*).

Metastatic disease to the liver remains a notable problem in treating oncological patients. The median survival for patients with liver metastases from colorectal cancer is 4–12 mo from the time of diagnosis of metastatic disease. The response rate to chemotherapy is highly variable (*4*). The standard chemotherapeutic agent used in these patients is fluorouracil (FU), which is applied as a continuous infusion or concomitant with modulators. Another approach often used in patients with inoperable liver metastases is the intra-arterial chemotherapy using a surgically implanted catheter in the gastroduodenal artery (*5*). Intra-arterial administration can increase drug concentrations at tumor sites and lower systemic drug exposure, as compared to the intravenous application. However, the studies published in the literature are not conclusive with respect to the therapeutic outcome (*6*).

Boyle et al. (*7*) evaluated the efficacy of intra-arterial therapy using FU and found response rates of 56% and a median survival time of 15 mo. Twenty percent of the patients survived longer than 3 yr. In contrast, De Takats et al. (*8*) reviewed the data obtained in patients with metastatic colorectal cancer receiving intra-arterial chemotherapy and noted significantly higher clinical response rates using the intra-arterial route, but they observed no benefit concerning the survival time. The highly variable results indicate the necessity to gain quantitative data about the pharmacokinetics of the cytostatic agent for each administration route.

Therefore, we investigated the intra-arterial treatment protocol using PET with ^{15}O-labeled water (^{15}O-water) as well as [^{18}F]fluorouracil (^{18}F-FU) in patients to examine the change in the access to the metastases as well as the pharmacokinetics of FU after intra-arterial and intravenous administration. We used ^{15}O-water, an inert tracer, for the evaluation of the access to the metastases. Oxygen-15-labeled water studies were performed immediately before the FU studies. One aim of the study was to compare the change in the access of the lesions after intra-arterial and intravenous administration using the inert tracer. Furthermore, we compared the change of the nonmetabolized tracer to the change of the transported and metabolized ^{18}F-FU after intra-arterial administration. Double examinations using ^{18}F-FU were used to gain quantitative data on the time–activity pattern of the labeled cytostatic agent in different tissues.

Our primary goal was to evaluate the distribution patterns of ^{18}F-FU in metastases, normal liver parenchyma and the aorta as

Received Oct. 9, 1996; revision accepted May 14, 1997.

For correspondence or reprints contact: Antonia Dimitrakopoulou-Strauss, MD, Department of Oncological Diagnostics and Therapy, German Cancer Research Center, Im Neuenheimer Feld 280, D-69120 Heidelberg, Germany.

a function of time after intravenous and intra-arterial administration of the drug. Furthermore, we compared the influx and the trapping of ^{18}F-FU for both administration routes.

MATERIALS AND METHODS

The final analysis comprised 30 examinations of 15 patients after intravenous and intra-arterial tracer administration. Fourteen patients included in this study suffered from nonresectable colorectal liver metastases and one patient refused resectional treatment. None of the patients had extrahepatic metastatic disease. None of them had undergone radiotherapy of the liver metastases. All patients had surgically implanted catheters (Infuse-a-Port; Infusaid Co., Norwood, MA) in the gastroduodenal artery and subcutaneous port systems. At laparotomy, liver metastases were confirmed by biopsy. Nonresectability and evidence for extrahepatic disease were checked.

The standard chemotherapeutic protocol included the infusion of FU (500 mg/m^2/24 hr for intravenous and 1500 mg/m^2/24 hr for intra-arterial therapy) for 5 days, followed by a 3-wk interval without treatment. None of the patients had previously received chemotherapy. The patients were examined with PET, either preceding the FU therapy or at least 1 wk after the last FU cycle in the therapy-free interval. The intravenous and the intra-arterial PET studies were performed within 5 days. Informed consent was obtained from all patients.

CT was used in all patients immediately before PET to identify the target area. We used contiguous 8-mm-thick cross sections and oral contrast enhancement, if required. Skin markings were made for proper repositioning of the patient for the PET study. Identical positioning supports were used for both CT and PET.

A positron emission tomograph with two ring detectors was used for the PET examinations. The system provided for the simultaneous acquisition of three slices: two primary sections and one cross-section. Each of the two rings, each of 107 cm diameter, contained 512 bismuth germanate-gadolinium orthosilicate detectors (crystal size = 6 mm × 20 mm × 30 mm) and provided a field of view of 52 mm. The mean sensitivity for the two primary sections was 12,500 cps/μCi/cm^3, and it was 17,500 cps/μCi/cm^3 for the secondary slice. The deadtime loss is 10% at 30,000 cps/slice. Transmission scans with more than 10 million counts per section were obtained with a rotating pin source before the first radionuclide application to obtain cross-sections for the attenuation correction of the acquired emission tomographic images.

The access to the metastatic lesions may be one limiting parameter for the FU accumulation. Therefore, we evaluated the access to the tumor lesions in 15 patients using the nonmetabolized tracer ^{15}O-water. The ^{15}O-water studies preceded the ^{18}F-FU studies. A minimum time interval of 10 min was used between the end of the ^{15}O-water study and the following ^{18}F-FU study. Oxygen-15 was produced using the procedure described by Del Fiore et al. (*9*). We injected 2960 MBq–3700 MBq ^{15}O-water before the ^{18}F-FU infusion, using the same administration route as for the ^{18}F-FU-study, and acquired five 1-min images after radiotracer injection.

The distribution and kinetics of ^{18}F-FU was investigated with ^{18}F-FU prepared by direct fluorination of uracil in acetic acid using (^{18}F)F_2 diluted in neon (*10*). Quality control included high-performance liquid chromatography. Typically, 17.5 mg of ^{18}F-FU with a purity greater than 99% and a specific activity of 1.14 × 10^{-5} Ci/μM were obtained. Fluorine-18-labeled FU (370–444 MBq) was given together with 500 mg unlabeled FU in a short 12-min infusion, either intravenously or intra-arterially via the implanted port system using an infusion pump. Immediately after the end of the ^{18}F-FU infusion, we infused physiological saline through the port system. Twelve 2-min images, followed by seven 5-min images and six 10-min images, beginning with the FU infusion, were acquired, for a total acquisition time of 120 min. Appropriate skin markings were used to align the system accurately with positioning laser lights.

PET cross-sections were reconstructed using an iterative reconstruction program based on a maximum likelihood algorithm with an image matrix of 256 × 256 due to the superior image quality (*11*). A 2-mm pixel size was chosen, and a resolution of 5.1 mm was obtained in the cross-sections of the patients. All images were corrected for scattered radiation, based on a modified procedure (*12*), and for attenuation (*13*). The PET cross-sections were compared with the corresponding CT slices as well as the transmission images to permit confident identification of the lesions by means of anatomic landmarks. Regions of interest (ROIs) were placed over the metastases, the normal liver parenchyma and the aorta. Only those metastases visible in two contiguous CT slices and identified in at least two consecutive PET slices were included in the final evaluation, to minimize partial volume effects. The slice showing the largest metastasis diameter was used for the placement of the ROI. Because small lesions visible in only one slice were excluded from the evaluation and respiration movement accounts for additional artifacts, no attempt was made to correct for the partial volume effect. The recovery coefficient was 88% for lesions with 1.5-cm diameter. Time-activity data were calculated from each image series for further quantitative evaluation.

Detailed quantitative evaluation of tracer kinetics requires the use of a compartment model. There are no accurate models available for either ^{15}O-water or ^{18}F-FU that can be applied to liver metastases. The most important problem in patient studies is the correct measurement of the input function, which requires arterial blood sampling. Another problem is the double supply of the liver through the hepatic artery and the portal vein. Therefore, we restricted quantitative evaluation to a semiquantitative approach using the calculation of the standardized uptake values (*1*): standardized uptake value (SUV) = tissue concentration (in MBq/g)/[injected dose (in MBq)/body weight (in g)].

For the evaluation of the ^{15}O-water intravenous studies, we used the 5-min SUV of the ^{15}O-water series as well as the integral uptake for the first 5 min [area under the curve (AUC)]. For the intra-arterial studies, we used the 1-min SUV as well as the integral uptake of the first 5 min (AUC). Area under the curve was calculated using the formula: AUC = (SUV·min). We chose ^{15}O-water, a freely diffusible, nonmetabolized tracer, for two reasons:

1. To compare the access to the metastatic lesions for both routes, based on the intravenous and intra-arterial administration of ^{15}O-water.
2. To compare the distribution of the nonmetabolized tracer with the kinetics of the transported and metabolized drug FU.

For the evaluation of the ^{18}F-FU studies, we used the uptake value 8 min after the end of the 12 min ^{18}F-FU infusion as a mass for the initial uptake of the nonmetabolized FU into the tumor cells (influx of the drug) and the uptake 120 min after onset of the ^{18}F-FU infusion for the evaluation of trapped FU. Therefore, the term influx is used to describe the initial uptake of nonmetabolized FU into the tumor cells, and the term trapping is used to describe the nonmetabolized intracellular amount of FU, which has not been eliminated out of the tumor cells until 2 hr after onset of the infusion. The data evaluation is based on the protocol described in a previous study (*3*).

For the statistical analysis of the data, we used the cluster analysis to identify groups of metastases with similar features (see Fig. 6). We chose Ward's method for the cluster analysis.

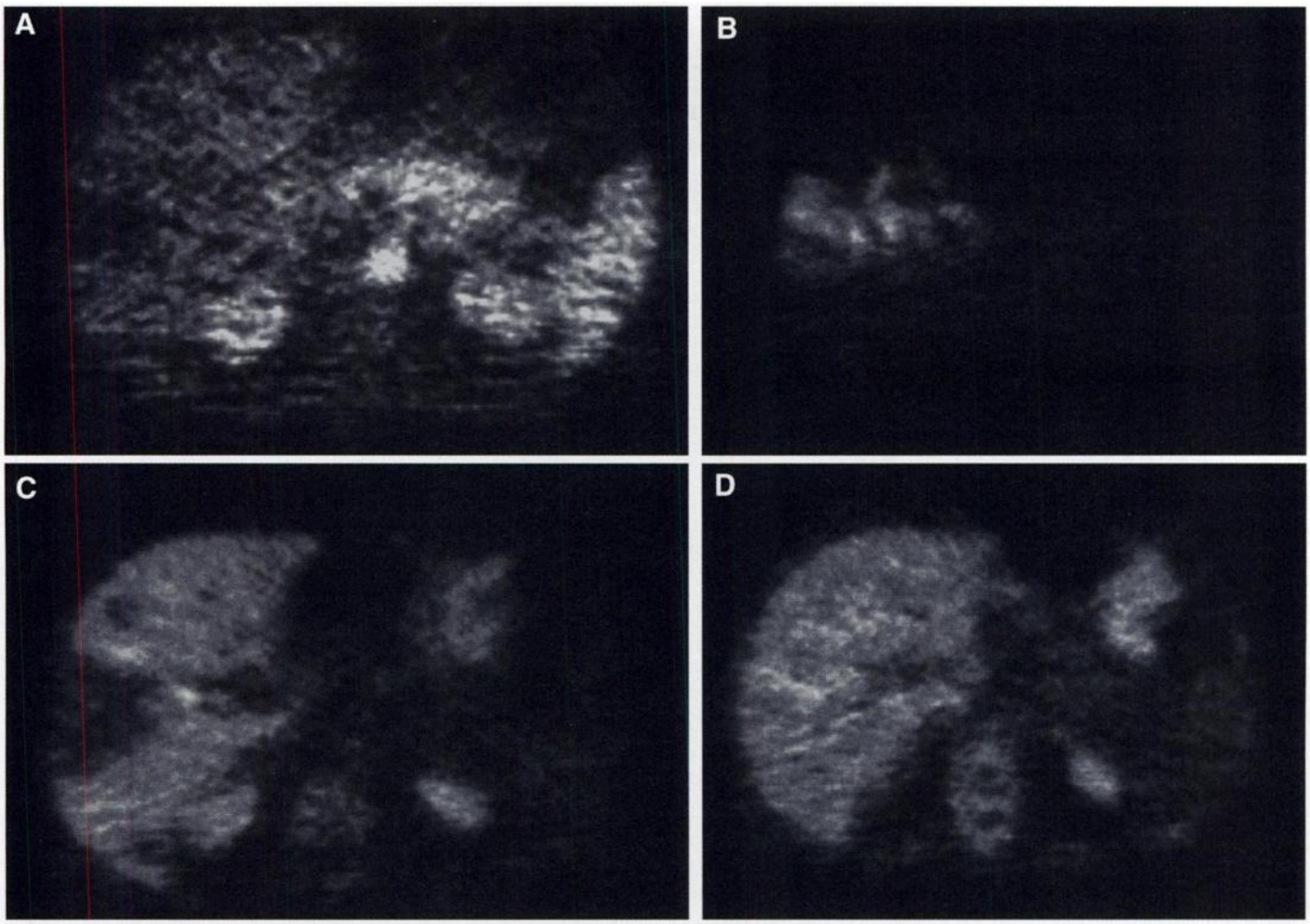

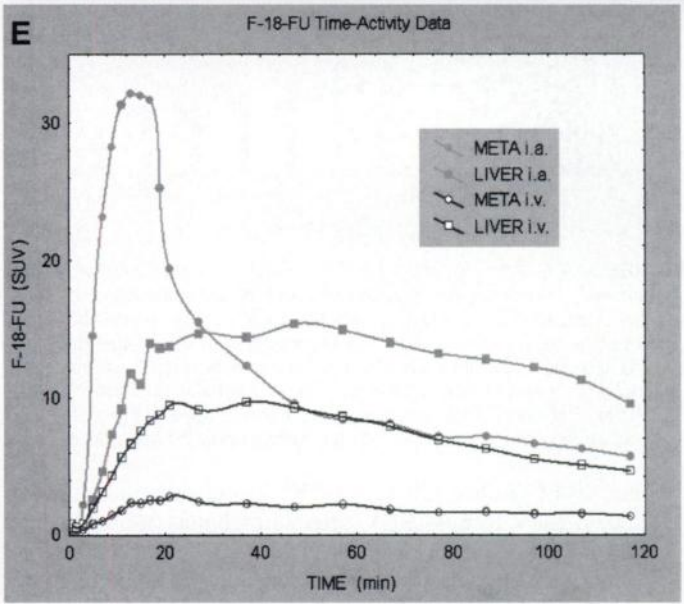

FIGURE 1. (A) PET cross-section 5 min after the intravenous application of ^{15}O-water in a patient with a liver metastasis from colorectal carcinoma in the lateral part of the right liver lobe. Decreased accumulation of the nonmetabolized tracer in the metastasis, in comparison to the normal liver parenchyma. (B) PET cross-section 1 min after the intra-arterial injection of ^{15}O-water in the patient in A. High, preferential accumulation of the nonmetabolized tracer in the metastasis in the lateral part of the right liver lobe, indicative of a better access and an enhanced perfusion of the lesion using the intra-arterial application. (C) PET cross-section 120 min after the intravenous application of ^{18}F-FU in the patient in A. The PET scan demonstrates a low accumulation of the labeled cytostatic agent in the metastasis in the lateral part of the right liver lobe, which is indicative of a low trapping of the tracer in the metastatic lesion. (D) PET cross-section 120 min after the intra-arterial application of ^{18}F-FU. The PET scan demonstrates nearly homogeneous distribution of the tracer in the metastasis, which cannot be delineated from the normal liver parenchyma. The intra-arterial application resulted in significantly higher ^{18}F-FU trapping. (E) Spline interpolated ^{18}F-FU time-activity data expressed in SUV for the metastasis and the normal liver parenchyma following intra-arterial as well as intravenous administration of the tracer. The intra-arterial infusion resulted in significantly higher ^{18}F-FU uptake values in the metastasis during the entire acquisition time.

RESULTS

Most of the liver metastases did not exhibit a significant ^{18}F-FU trapping on the PET images and were delineated as defects against the normal liver parenchyma 120 min postinjection. The visual inspection of the ^{18}F-FU images revealed a significant difference in the ^{18}F-FU trapping for the intravenous and intra-arterial administration in only two patients. Figure 1 demonstrates an example of a liver metastasis showing a significant enhancement in the FU trapping after intra-arterial administration. Furthermore, the access and, therefore, the perfusion of the lesion were different for the two administration routes. Although the intravenous administration of ^{15}O-water failed to show a preferential tracer uptake in the metastasis (Fig. 1A), the intra-arterial application of ^{15}O-water through the implanted port revealed a segmental perfusion of the liver, including the metastasis in the right lateral part (Fig. 1B). We measured high concentration values for ^{15}O-water and high ^{18}F-FU influx and trapping after onset of the intra-arterial

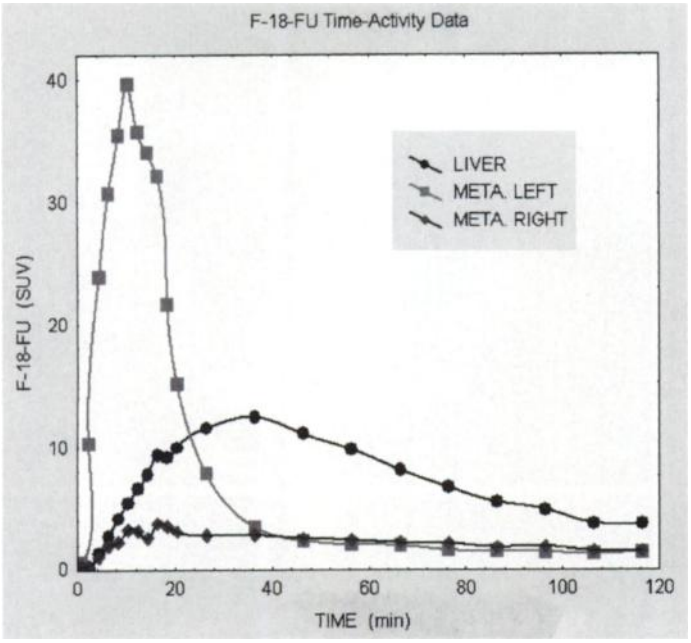

FIGURE 2. Spline interpolated PET time-activity data for ^{18}F-FU (in SUV) in a patient with two liver metastases (one in the left and a second in the right liver lobe) from colorectal carcinoma. For comparison, the data in the normal liver parenchyma are also shown. Note the discrepancies in the pharmacokinetic patterns of ^{18}F-FU, even in the same patient. The lesion in the left lower lobe showed a very high accumulation shortly after the intra-arterial ^{18}F-FU infusion, followed by a rapid decrease of the uptake values, whereas the metastasis in the right liver lobe demonstrated low ^{18}F-FU concentrations during the entire acquisition time. This seems to be indicative of a different transport system in each metastasis.

^{18}F-FU infusion. The quantitative evaluation demonstrated a 3.8-fold higher ^{18}F-FU trapping (Fig. 1E) after the intra-arterial infusion of the cytostatic agent in the patient of Figure 1. The data show that intra-arterial administration resulted in better access and in an enhancement of the ^{18}F-FU influx and trapping of the radiolabeled drug. However, the change in access, as measured by ^{15}O-water, was significantly higher than the change in the ^{18}F-FU trapping in the metastasis.

The ^{18}F-FU time-activity data were significantly different in most of the patients after intra-arterial administration. We noted large differences in the ^{18}F-FU distribution patterns for metastases even in the same patient. Figure 2 demonstrates a representative example of two metastases in the same patient showing a different FU influx and FU trapping. Although the access through the catheter in the gastroduodenal artery was comparable and high for both metastases, the metastasis in the right liver lobe showed a low FU influx (3.1 SUV), followed by a low FU trapping (1.5 SUV). In contrast, the lesion in the left liver lobe showed an extremely high FU influx (39.6 SUV) followed by a steep decline of the activity concentration and a low FU trapping of 1.4 SUV, due to the very high elimination rate. This example demonstrates that an improved access to a metastasis does not necessarily lead to an increased FU trapping.

The final evaluation comprised 24 metastases in 15 patients (Fig. 3). The variation of the ^{18}F-FU concentrations was higher after the intra-arterial application of the cytostatic drug. The tracer concentrations in the metastatic lesions were lower than the ^{18}F-FU concentrations in the normal liver parenchyma after the intravenous application (Fig. 3A). Intra-arterial tracer administration resulted in enhanced ^{18}F-FU concentrations in some lesions within 20 min after onset of the infusion, due to the improved access (Fig. 3B).

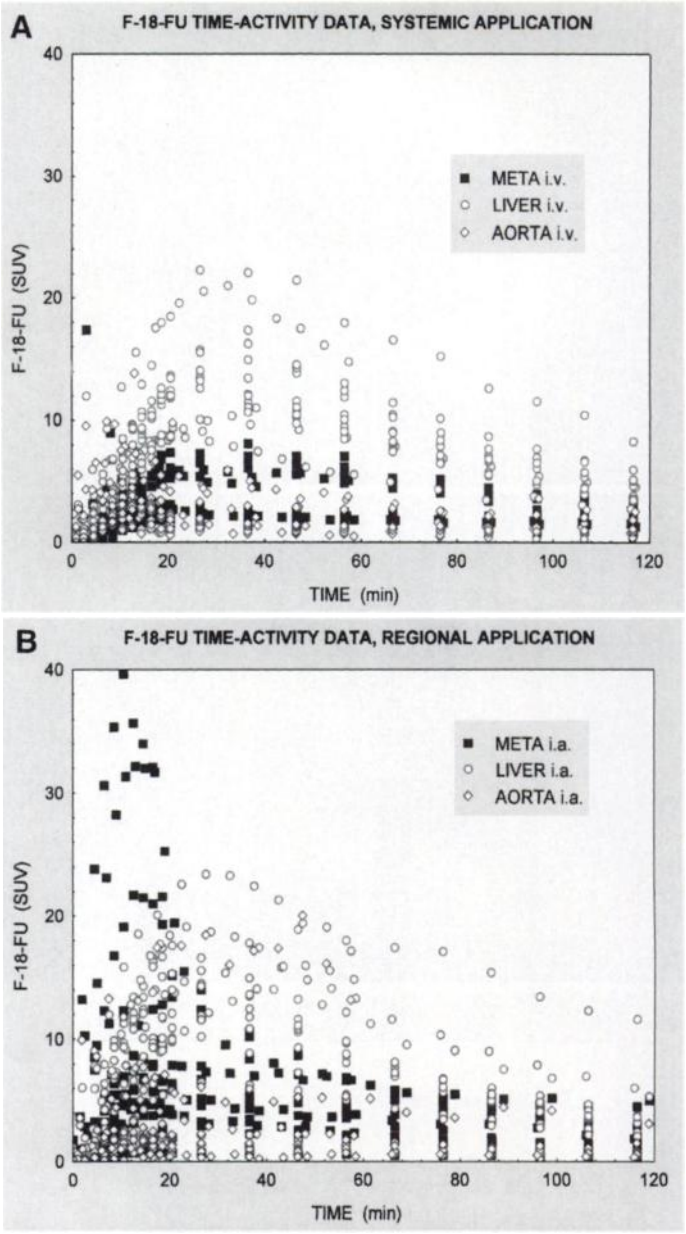

FIGURE 3. (A) Scatter plot of the ^{18}F-FU time-activity data (SUV) for the liver metastases, the normal liver parenchyma and the aorta following the intravenous application of ^{18}F-FU in all patients. Liver metastases demonstrated lower uptake values than the normal liver parenchyma. (B) Scatter plot of the ^{18}F-FU time-activity data (SUV) for the liver metastases, the normal liver parenchyma and the aorta following the intra-arterial application of the ^{18}F-FU in all patients. High variation of the tracer uptake in the metastases with enhanced uptake values in the early phase up to 20 min postinjection.

The ^{18}F-FU influx (20 min SUV) in the metastases varied from 0.96 SUV to 6.08 SUV after intravenous administration and from 0.61 SUV to 18.75 SUV after intra-arterial administration. A lesion-to-lesion comparison of the ^{18}F-FU influx demonstrated that 20 of 24 metastases had higher ^{18}F-FU influx after intra-arterial drug administration (Fig. 4). The ratio between the ^{18}F-FU influx measured in the metastases after intra-arterial and the intravenous administration varied between 0.24 and 13.3, with a median value of 2.3.

The ^{18}F-FU trapping (120-min SUV) in the metastases varied from 0.38 SUV to 3.89 SUV after intravenous administration and from 0.35 SUV to 5.03 SUV after intra-arterial administration. The highest ^{18}F-FU trapping values were noted after the intra-arterial infusion of the radiolabeled drug. A lesion-to-lesion comparison of the ^{18}F-FU uptake 120 min postinjection

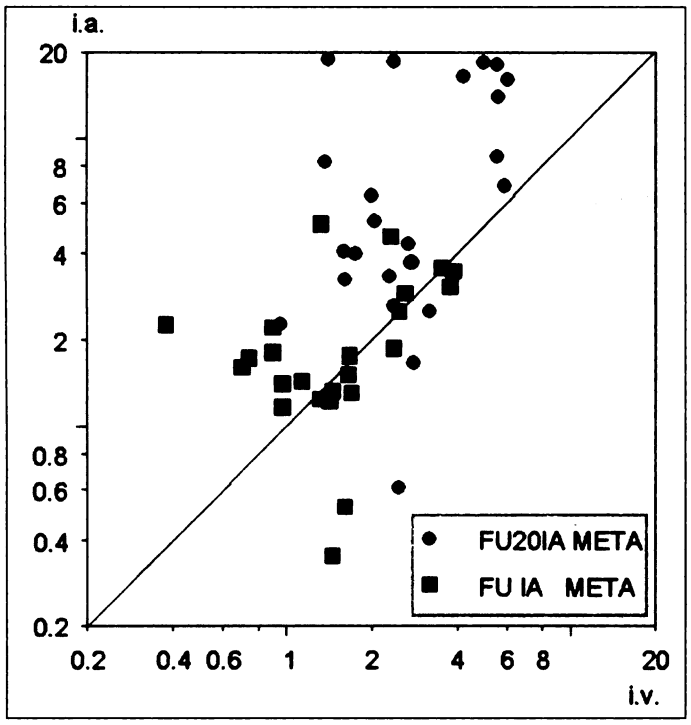

FIGURE 4. Comparison of the intravenous and intra-arterial administration for the ^{18}F-FU influx (FU2OIA META) and the ^{18}F-FU trapping (FU IA META) in the metastases. The uptake is expressed in SUV. Twenty of 24 lesions showed an enhanced influx, and 8 of 24 showed an enhanced trapping of the drug when intra-arterial administration was used.

demonstrated 8 of 24 metastases with a higher ^{18}F-FU trapping after the intra-arterial administration (Fig. 4). The ratio between the ^{18}F-FU trapping measured in the metastases after intra-arterial and intravenous administration of the tracer varied between 0.24 and 5.92, with a median value of 1.03.

The access to the lesions was measured with ^{15}O-water, a nonmetabolized tracer, and was significantly higher for all metastases using the intra-arterial administration. The ^{15}Oconcentration values for the metastases ranged from 16.25 SUV·min to 217.40 SUV·min for the intra-arterial and from 6.47 SUV·min to 51.00 SUV·min for the intravenous application route. Intra-arterial application led to a better access in 21 of 24 metastases. The ratio between the AUC values (expressed in SUV·min), measured in the metastases after intra-arterial and intravenous application of ^{15}O-water, varied between 0.04 and 18.73, with a median value of 5.15.

A comparison of the ^{15}O-water-distribution values and the ^{18}F-FU influx using both administration routes is demonstrated on Figure 5A. The data show that the change in the access to the metastases parallels the change of the ^{18}F-FU influx. A comparison of the ^{15}O-water distribution values of the metastases with the ^{18}F-FU trapping indicates that 12 of 24 lesions showed similar ^{18}F-FU trapping values for both application routes, whereas 4 of 24 achieved lower ^{18}F-FU trapping values using the intra-arterial application (Fig. 5B). The data show that ^{18}F-FU trapping does not correlate with changes of the access, despite the fact that the ^{18}F-FU influx is strongly dependent on the access to the lesions.

A comparison of the AUC values for the ^{15}O-water, the ^{18}F-FU influx and the ^{18}F-FU trapping in the metastases using the intravenous application is demonstrated in Figure 6. There is no statistically significant linear correlation between the ^{15}O-water and the ^{18}F-FU influx ($r = 0.25$, $p < 0.05$), nor is there a correlation between ^{15}O-water and ^{18}F-FU trapping ($r = 0.01$, $p < 0.05$). Cluster analysis (Ward's method) for the

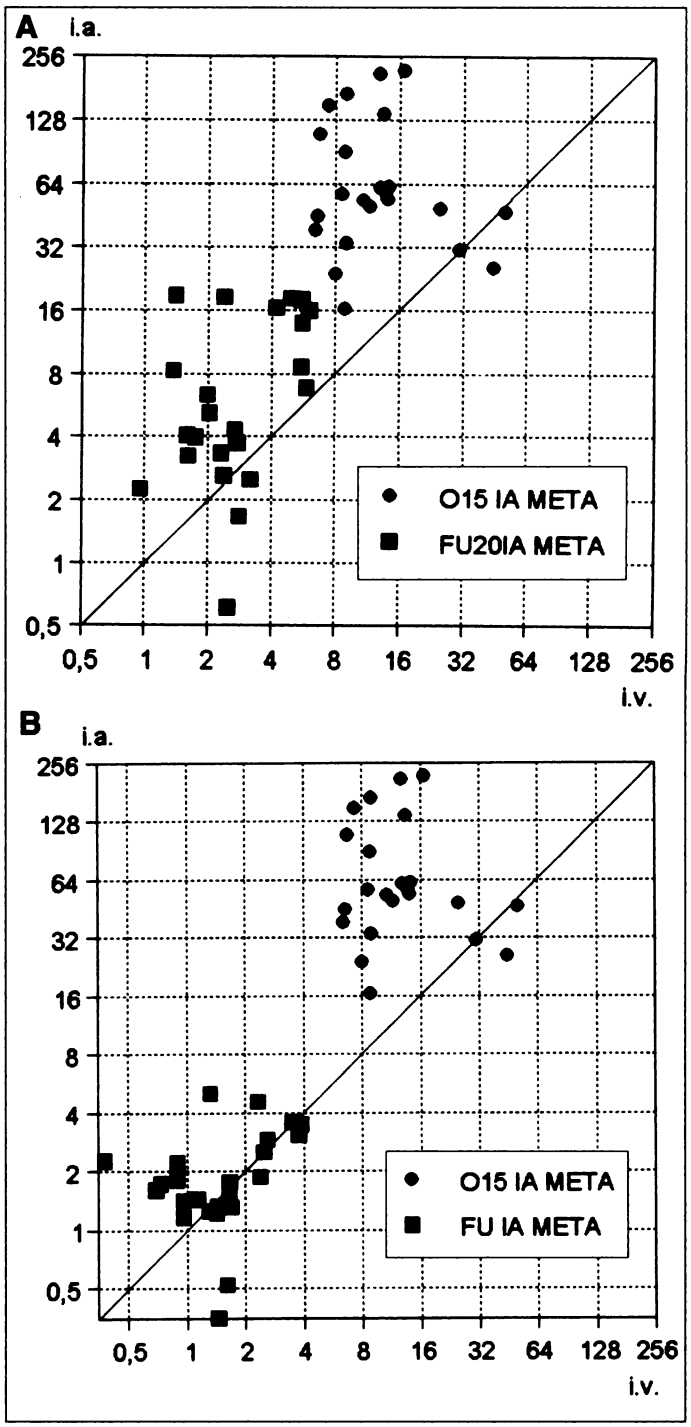

FIGURE 5. (A) Comparison of the distribution of the nonmetabolized tracer ^{15}O-water (AUC) and the ^{18}F-FU influx (20 min ^{18}F-FU SUV) for the intravenous and the intra-arterial application in all metastases. There is a match between the improvement in the access to the metastases, as measured by ^{15}O-water and the ^{18}F-FU influx. (B) Comparison of the distribution of the nonmetabolized tracer ^{15}O-water (AUC) and the ^{18}F-FU trapping (120 min ^{18}F-FU SUV) for the intravenous and the intra-arterial application in all metastases. There is a mismatch between the improvement in the access to the metastases, as measured by ^{15}O-water and the ^{18}F-FU trapping. Fifty percent of the lesions showed similar trapping values for ^{18}F-FU following intra-arterial administration.

^{15}O-water and the ^{18}F-FU influx revealed three clusters. Cluster I included six lesions with low ^{15}O-water distribution values, high ^{18}F-FU influx and high ^{18}F-FU trapping. Cluster II included four lesions with high ^{15}O-water distribution values, intermediate to high ^{18}F-FU influx and intermediate to high ^{18}F-FU trapping. A correlation of $r = 0.77$ ($p < 0.05$) was

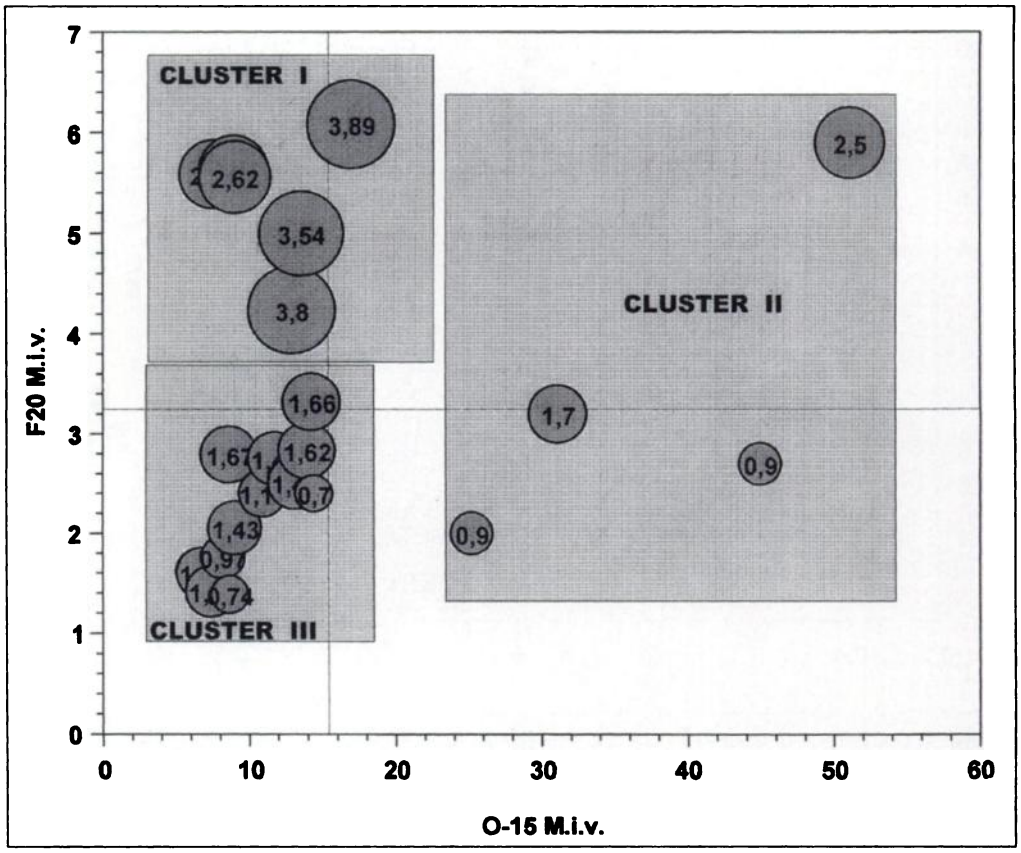

FIGURE 6. Comparison of the accumulation (AUC) of the nonmetabolized tracer ^{15}O-water (^{15}O M.i.v.), the ^{18}F-FU influx (F20 M.i.v.) and ^{18}F-FU trapping (F120 M.i.v.) in all metastases following intravenous administration. The circles represent ^{18}F-FU trapping. Cluster analysis identified three groups, as follows: Cluster I (n = 6), low ^{15}O-water distribution values, high ^{18}F-FU influx and high ^{18}F-FU trapping (>2.0 SUV) and no correlation between ^{15}O-water and ^{18}F-FU influx; Cluster II (n = 4), high ^{15}O-water distribution values, intermediate to high ^{18}F-FU influx and low ^{18}F-FU trapping (only one lesion with FU trapping >2.0 SUV) and significant correlation ($r = 0.77$, $p < 0.05$) between ^{15}O-water and ^{18}F-FU influx; and Cluster III (n = 14), low ^{15}O-water distribution values, low ^{18}F-FU influx and low ^{18}F-FU trapping (<2.0 SUV) and significant correlation ($r = 0.54$, $p < 0.05$) between ^{15}O-water and ^{18}F-FU influx.

found for ^{15}O-water and ^{18}F-FU influx in Cluster II. Cluster III comprised the rest of the lesions (n = 14) with low ^{15}O-water distribution values, low ^{18}F-FU influx and low ^{18}F-FU trapping. There is a significant linear correlation between the parameters in Cluster III, with $r = 0.54$ ($p < 0.05$). Interestingly, the metastases identified in Cluster I showed the highest ^{18}F-FU trapping, ranging from 2.34 SUV to 3.89 SUV. Although all six lesions of Cluster I demonstrated a ^{18}F-FU trapping greater than 2.0 SUV, only one of four lesions included in Cluster II and none of the lesions in Cluster III achieved ^{18}F-FU trapping values greater than 2.0 SUV. The data demonstrate that the ^{18}F-FU influx is dependent on the access in 18 of 24 (75%) of the metastases. In contrast, enhanced ^{18}F-FU trapping was exclusively observed only in the minority of lesions (n = 6), without any correlation between ^{15}O-water and ^{18}F-FU influx (Cluster I).

Furthermore, we compared the ^{18}F-FU trapping in the lesions of Cluster I for both administration routes. Intra-arterial administration enhanced the ^{18}F-FU trapping in only one metastasis. Four of the lesions in Cluster I showed a comparable ^{18}F-FU trapping, and in one metastasis, there was a decrease of the ^{18}F-FU trapping after the intra-arterial application. Intra-arterial drug administration enhanced the ^{18}F-FU trapping in 2 of 4 metastases of Cluster II and in 7 of 14 metastases of Cluster III.

DISCUSSION

Hepatic arterial chemotherapy has been practiced for the past 20 yr for therapy of metastatic liver disease (*5,7,8*). Regional drug delivery is a promising approach designed to improve selectivity and efficacy of chemotherapy because regional delivery can potentially increase drug concentrations at tumor sites and lower systemic toxicity. In the 1980s, improved technologies, like implantable pumps and dedicated catheters, were developed, which contributed to a proliferation of regional delivery studies. Clinical studies have been performed in several patients with liver metastases from colorectal cancer using either 5-FU or modified treatment protocols with modulators such as folinic acid or other cytostatic agents (*4*). The results of these clinical trials were highly variable, and the mean survival time was equivalent to the systemic application. In a few cases, some authors reported even a complete response using intra-arterial application, but the results could not be verified in larger patient collectives (*4–6*). The major response criteria routinely used are the change in tumor volume, the serum level of tumor markers and the survival time after onset of therapy. The major limitation of these response criteria is the assumption that multiple metastases in the same patient will evoke equivalent responses. This is not necessarily the case, as demonstrated in Figure 2. Therefore, we like to emphasize the use of individual growth rates for the evaluation of the therapeutic effect.

Because all forms of intra-arterial delivery are more complex than intravenous application, a careful assessment of the expected benefit should be made, which means that a pharmacokinetic analysis is necessary to evaluate or even predict the effect of this approach, in comparison to the classic systemic application. Furthermore, because intra-arterial application is only suitable if a drug has already shown a cytostatic effect in the systemic setting of application, the goal of intra-arterial application would be to push some partial responses to complete response and some minimal response into at least partial response. Another problem concerning the intra-arterial drug administration is the question of the tumor perfusion. Although the normal liver parenchyma receives 25% of its blood supply from the hepatic artery and the remainder from the portal vein, it is generally accepted that liver metastases derive their blood supply from the hepatic artery. It also accepted that there may be differences in the vascularity of tumors because it is possible that small metastases can receive their blood supply from the

portal vein exclusively. For this purpose, it is helpful to examine the perfusion and the access to a metastatic lesion prior onset to intra-arterial chemotherapy and, furthermore, to assess individual drug pharmacokinetics at the target area using the same application route as for therapy (*3*).

Several methods have been proposed to evaluate the distribution of a chemotherapeutic agent after intra-arterial application, such as percutaneous arteriography, intraoperative use of fluorescent dyes and hepatic artery perfusion scintigraphy with ^{99m}Tc-labeled macroaggregated albumin (^{99m}Tc-MAA). In the past 10 yr, radionuclide techniques, such as perfusion studies with ^{99m}Tc-MAA, were recommended not only to check the catheter position but also to assess the perfusion pattern using the same port system for the application of the radiopharmaceutical (*14*). Some authors attempted to predict therapy outcome with the MAA perfusion studies. The reported results are highly divergent. Kaplan et al. (*15*) were able to predict therapy response in 10 of 11 patients using ^{99m}Tc-MAA perfusion scintigraphy. However, these promising data could not be confirmed in a larger patient collective. Furthermore, Lehner et al. (*16*), in a detailed study, evaluated the relationship between the perfusion of the metastases, as measured with MAA, and the survival time and emphasized that no significant correlation between these two parameters exists. It was not possible to recognize responders from nonresponders using the MAA data alone.

Labeled particles are suitable to trace the position of the catheter, but they provide only an inaccurate map of the distribution of the liver perfusion. Another limitation of the use of MAA for liver perfusion studies is the fact that this tracer can only be used through the intra-arterial route and a comparison of the access between intra-arterial and intravenous administration is not possible. Furthermore, due to the conventional imaging, only a qualitative evaluation of the tracer uptake is possible. We used ^{15}O-water, a freely diffusible tracer, which provides information about the distribution of a nonmetabolized tracer. Oxygen-15-labeled water has been used primarily for perfusion studies in the brain because the distribution of this tracer reflects the tissue perfusion at the capillary level, due to the small size of the water molecule. Herscovitch et al. (*17*), in their excellent experimental study, reported a linear correlation between the tissue radioactivity measured in the first 40 sec in a ROI, as measured with PET and ^{15}O-water and relative differences in flow. All these considerations are true only for the intravenous application of the tracer and have been well documented for brain studies. It is still an open question if the ^{15}O concentration in a tumor is proportional to blood flow. We chose ^{15}O-water in this setting for two reasons. First, to evaluate the access to the metastatic lesions for both administration routes, and second, to compare the distribution of a small molecule that was not further metabolized to the metabolized tracer ^{18}F-FU. Using the intravenous application of the ^{15}O-water, the 1-min images are blood flow-weighted, whereas the 4- to 5-min images are more dominated by the distribution volume of the water. When the intra-arterial administration of the ^{15}O-water is used, the PET images are primarily blood volume-weighted. We used the 4- to 5-min SUV for the evaluation of the intravenous administration and the 1-min SUV for the evaluation of the intra-arterial administration, as well as the AUC to compare the distribution volume of the tracer using each administration route, because both parameters are dominated by the volume of the distribution of water and contain less flow information.

Furthermore, we compared the intravenous to the intra-arterial application to gain data about the change in the access to the lesions. We noted higher AUC values in 21 of 24 (87.5%) metastases using the intra-arterial approach, which indicates a higher distribution volume and, therefore, an improvement in the access of the lesions. These data confirm the pharmacological considerations about the use of the intra-arterial application (*18*). The significantly higher ^{15}O concentration measured in the tumor after the intra-arterial tracer injection as compared to the surrounding liver tissue suggests a higher arterial perfusion of the tumor than of the liver. This advantage is important for the intra-arterial chemotherapy because it is in accordance to the theoretical considerations concerning the preferential arterial perfusion of liver metastases and a lower toxicity and side effects for the normal liver parenchyma. However, a prerequisite for lower toxicity is a high first-pass extraction of the FU, which was not noted in the lesions evaluated in this study.

In some cases, as in the patient shown in Figure 1, intra-arterial administration may result in a preferential distribution of the ^{15}O-water in a liver segment. This finding was consistent with a second water study performed in this patient a week later. Bledin et al. (*19*) also noted segmental distribution patterns, using ^{99m}Tc-MAA through an angiographically placed catheter, when catheters were placed proximal to the bifurcation of a vessel. The author was able to overcome the segmental distribution with a pulsatile pump, which does not allow laminar flow to occur. In this study, we did not try to overcome the segmental distribution because all liver metastases were confined to the accessed liver segments, as in the patient shown in Figure 1, who was a responder.

The pharmacokinetics of FU was examined after intra-arterial and intravenous administration in the same patients using the same dose of nonlabeled FU. PET with ^{18}F-FU enables direct measurement of the kinetics of the cytostatic agent because ^{18}F-FU is a biochemical that is identical to the nonlabeled drug. One critical point is the selection of the appropriate time intervals for the evaluation of pharmacokinetic parameters of the FU data, like the FU transport or influx of the drug and the trapping of the cytostatic agent. We showed in a previous work that early FU uptake values (20 min postinjection) reflect the FU transport or the influx of the drug and late FU uptake values (120 min) represent the amount of trapped nonmetabolized FU when intravenous administration is used (*3,20,21*). Chaudhuri et al. (*22*) examined the FU pathway in mice bearing sarcoma-180 and reported that, even 60 min after injection of 25 mg/kg FU, 61% of the radioactivity in the tumor represents nonmetabolized FU. Therefore, PET images obtained 8 min after the end of the 12-min intravenous ^{18}F-FU infusion represent the amount of the influx of the drug and can be used as a mass for the FU transport. Late images obtained 120 min after the systemic ^{18}F-FU administration most probably represent trapped nonmetabolized FU. Wolf et al. (*23*) studied the kinetics of FU in some patients as well as in rabbits bearing VX2 tumors using ^{19}F magnetic resonance spectroscopy up to 120 min postinjection. He noted a significant trapping of nonmetabolized FU in some human tumors. Furthermore, the amount of trapped FU correlated with therapy outcome. Shani and Wolf (*24*) examined the FU uptake in two variants of the same tumor in mice: in the solid L-1210 lymphocytic leukemia tumor, susceptible to FU, and in a tumor line resistant to FU. They noted mean tumor-to-blood ratios of 1.9 2 hr after intravenous FU injection in the sensitive line and of 0.96 in the resistant tumor. The difference was even greater 12 hr postinjection, with ratios of 20.69 for the sensitive and 4.04 for the resistant tumors, respectively (*24*). The data support the hypothesis that tumor response is associated with high FU uptake in the late phase, at least 1 hr after the FU application. Further-

more, the ^{18}F-FU signal measured by PET 120 min postinjection must primarily reflect nonmetabolized FU or FU metabolites. It should be noted that inactive FU catabolites, like α-fluoro-β-alanine have only been detected in the normal liver parenchyma, not in the metastases (*25*). These data suggest that the ^{18}F-FU uptake values measured 20 min and 120 min postinjection are most helpful for the therapy management in individual patients.

In this study, the highest ^{18}F-FU concentrations were measured after the intra-arterial administration, with maximum uptakes of 18.75 SUV for ^{18}F-FU influx and of 5.03 SUV for ^{18}F-FU trapping. In contrast, intravenous administration demonstrated significantly lower maximas with 6.08 SUV for the ^{18}F-FU influx and 3.89 SUV for the ^{18}F-FU trapping. A comparison of the ^{18}F-FU influx showed higher uptake values in 20 of 24 (83.3%) of the evaluated lesions. The distribution volume of the ^{15}O-water (AUC) was higher for 21 of 24 (87.5%) of the metastases after intra-arterial administration. Although the access to the metastases was enhanced by a factor of 5 (median value), the influx of the drug was enhanced by a factor of 2.3 (median value) through the intra-arterial route. These data can be explained by a higher concentration at the tumor site, due to the intra-arterial administration. The effect is higher for the ^{15}O-water than for the ^{18}F-FU, due to exchange during recirculation and the size of the molecule. Regardless of the improved access and enhanced ^{18}F-FU influx, there was no improvement of the FU trapping (median = 1.03 SUV). An enhanced trapping of the agent was noted in one-third (8 of 24) of all metastases. Therefore, the cytostatic agent is eliminated very quickly out of the tumor cells, despite the better access and the enhanced local concentration of the drug in the early phase. Several lesions showed an improved influx of the drug after intra-arterial application, but the major limiting parameter for an enhanced trapping is the very high elimination of FU out of the tumor cells, which was not saturated with the FU dose used in patients.

Elimination of FU seems to be the most important limiting parameter for the therapy response and may explain the relative drug resistance noted in most patients with metastatic colorectal cancer in the clinical routine. The influx transport constant for FU is too low, as compared to the efflux transport constant, which does not seem to be saturated after intra-arterial application with the regular FU doses used for treatment in patients. This may be related to the intrinsic multidrug resistance (MDR) which is frequently associated with an enhanced amount of the P-glycoprotein (Pgp), encoded by the *MDR1* gene. The role of Pgp for the MDR in colorectal cancer is supported by the experimental data from Sela et al. (*26*), who investigated the modulation of MDR by liposome-encapsulated vincristine in a drug-resistant human colon cancer cell line HT-29 (super-*MRD1*) and the potentiation of this modulation in combination with monoclonal antibody MRK-16 or verapamil. They noted a ten-fold potentiation of the cytotoxicity using the combination of the MRK-16 and liposome-encapsulated vincristine. However, it is unclear what the the clinical relevance of drug resistance in metastatic colorectal cancer is and how to overcome it. Furthermore, there is also an open question of whether the use of modulators of the MDR concomitant to FU can help to decrease the efflux transport constant of the agent effectively and, therefore, contribute to an enhanced FU trapping. Another possibility may be the use of oligonucleotides to block the Pgp and indirectly reduce the elimination.

The transport of FU has been examined in a variety of cell and tissue types with different results. The transport of FU in cultured cells reportedly occurs through a nonconcentrative, saturable mechanism; furthermore, through an active, concentrative mechanism; or through nonfacilitated diffusion (*27–30*). Transport of FU by intestinal preparations was by both a saturable and a nonsaturable process, with the saturable process being active, concentrative and sodium-dependent. We tried to evaluate the transport mechanisms and compared the ^{15}O-water distribution of the metastases, the ^{18}F-FU influx and the ^{18}F-FU trapping exclusively using the data from the intravenous studies. The evaluation of the data using cluster analysis revealed a group of six metastases (Cluster I) with low ^{15}O-water distribution values, high ^{18}F-FU influx and high ^{18}F-FU trapping. An explanation of this phenomenon may be a nonperfusion-dependent transport system. To support this theory, we compared the data of these metastases after intra-arterial application and found that only one of six (16.6%) metastases showed enhanced ^{18}F-FU trapping. Cluster analysis revealed a second group, including 14 metastases (Cluster III), with a perfusion-dependent transport, showing a significant correlation ($r = 0.54$, $p < 0.05$) between ^{15}O-water and FU influx after the intravenous application. In contrast to Cluster I, 7 of 14 (50%) of the metastases included in Cluster III showed an improvement in the FU trapping after the intra-arterial administration. Therefore, it is likely that a saturable transport system exists, which limits the profit from the enhanced FU dose in the target area, like in the lesions of Cluster I. The data demonstrate that PET studies enable a noninvasive assessment of the transport system of the FU, using the same administration route as for therapy.

It is not possible to predict the pharmacokinetics of FU after intra-arterial administration using only an intravenous PET study. However, it may be possible to exclude patients from intra-arterial treatment if they have an nonperfusion-dependent FU transport system (Cluster I) because they are not likely to profit from the intra-arterial approach. For this reason, a PET study through a super-selectively placed angiographic catheter before surgery, for example, is recommended to examine the kinetics of the drug.

PET studies with ^{15}O-water and ^{18}F-FU are a useful tool for therapy management in patients with metastatic colorectal cancer and can help to optimize and individualize the chemotherapeutic treatment. The use of ^{18}F-FU is superior to metabolically active tracers like FDG because one ^{18}F-FU study reflects the distribution of the cytostatic agent, the transport pattern as well as the trapping.

CONCLUSION

Studies with ^{18}F-FU in patients with metastatic colorectal carcinomas have shown that PET is a suitable tool for pharmacokinetic studies in the target area. Furthermore, it is possible to compare different application routes. In this study, we compared the intravenous and intra-arterial administration of ^{18}F-FU because ^{18}F-labeled FU is identical to the nonlabeled agent.

Intra-arterial administration improved the access in 21 of 24 (87.5%) of the metastases. We noted an enhancement of the ^{18}F-FU influx in 20 of 24 (83.3%) of the lesions. An enhanced ^{18}F-FU trapping was observed in 8 of 24 (33.3%) of the lesions using the intra-arterial route of application. The data demonstrate that, despite the improvement of the access to the metastases by a factor of 5 (median value) and the enhancement of ^{18}F-FU influx by a factor of 2.3 (median value), the ^{18}F-FU trapping was not improved (median = 1.03 SUV). Therefore, the major limiting parameter for the low therapeutic effect of the intra-arterial FU chemotherapy is the very high elimination of the drug out of the tumor cells.

An intravenous PET study with ^{18}F-FU cannot be used for

prediction of the pharmacokinetics of the drug after the intra-arterial administration.

Cluster analysis of the intravenous ^{15}O-water data, the ^{18}F-FU influx data and the ^{18}F-FU trapping data revealed at least two different transport systems of FU. A nonperfusion-dependent transport system was noted in 6 of 24 lesions. The data support the hypothesis that PET double-tracer studies can be used to select lesions showing a nonperfusion-dependent transport system and exclude them from the intra-arterial chemotherapy.

REFERENCES

1. Strauss LG, Clorius JH, Schlag P, et al. Recurrence of colorectal tumors: PET evaluation. *Radiology* 1989;170:329–332.
2. Strauss LG, Conti PS. The applications of PET in clinical oncology. *J Nucl Med* 1991;32:623–648.
3. Dimitrakopoulou A, Strauss LG, Clorius JH, et al. Studies with positron emission tomography after systemic administration of fluorine-18-uracil in patients with liver metastases from colorectal carcinoma. *J Nucl Med* 1993;34:1075–1081.
4. Kemeny N. The systemic chemotherapy of hepatic metastases. *Semin Oncol* 1983;10: 148–158.
5. Niederhuber JE, Ensminger WD. Surgical consideration in the management of hepatic neoplasia. *Semin Oncol* 1983;10:135–147.
6. Vaughn DJ, Haller DG. Nonsurgical management of recurrent colorectal cancer. *Cancer* 1993;71:4278–4292.
7. Boyle FM, Smith RC, Levi JA. Continuous hepatic artery infusion of 5-fluorouracil for metastatic colorectal cancer localised to the liver. *Aust N Z J Med* 1993;23:32–34.
8. De Takats PG, Kerr DJ, Poole CJ, et al. Hepatic arterial chemotherapy for metastatic colorectal carcinoma. *Br J Cancer* 1994;69:372–378.
9. Del Fiore F, Depresseux JC, Bartsch P, Quaglia L, Peters JM. Production of oxygen-15, nitrogen-13 and carbon-11 and of their low molecular weight derivatives for biomedical applications. *Int J Appl Radiat Isot* 1979;30:5443–5449.
10. Oberdorfer F, Hofmann E, Maier-Borst W. Preparation of 18-F-labeled 5-fluorouracil of very high purity. *J Label Compd Radiopharm* 1989;27:137–145.
11. Doll J, Ostertag HJ, Bellemann ME, et al. Effects of distorted PET projection data on the reconstructed image using different reconstruction algorithms. In: Bergmann H, Sinzinger H, eds. *Radioactive isotopes in clinical medicine and research advances in pharmacological sciences*. Basel: Birkhäuser Verlag; 1995:85–90.
12. Hoverath H, Kübler WK, Ostertag H, et al. Scatter correction in the transaxial slices of a whole-body positron emission tomograph. *Phys Med Biol* 1993;38:717–728.
13. Ostertag H, Kübler WK, Doll J, Lorenz WJ. Measured attenuation correction methods. *Eur J Nucl Med* 1989;15:722–726.
14. Ziessman HA, Thrall JH, Gyves JW, et al. Quantitative hepatic arterial perfusion scintigraphy and starch microspheres in cancer chemotherapy. *J Nucl Med* 1983;24: 871–875.
15. Kaplan WD, Jaroszweski J, Clarke R, et al. Radionuclide angiography to predict patient response to hepatic artery chemotherapy. *Cancer Treat Rep* 1980;64:1217–1222.
16. Lehner B, Kretzschmar U, Bubeck B, et al. Results of liver angiography and perfusion scintigraphy do not correlate with response to hepatic artery infusion chemotherapy. *J Surg Oncol* 1988;39:73–78.
17. Herscovitch P, Markham J, Raichle ME. Brain blood flow measured with intravenous $H_2{}^{15}O$. I. Theory and error analysis. *J Nucl Med* 1983;24:782–789.
18. Collins J. Pharmacologic rationale for regional drug delivery (review). *J Clin Oncol* 1984;2:498–504.
19. Bledin AG, Kim EE, Chuang VP, et al. Changes of arterial blood flow patterns during infusion chemotherapy, as monitored by intra-arterially injected technetium-99m macroaggregated albumin. *Br J Radiol* 1984;57:197–203.
20. Dimitrakopoulou A, Strauss LG, Knopp MV, et al. Positron emission tomography measurement of fluorouracil uptake prior to therapy and chemotherapy response. In: Breit A, Heuck A, Lukas P, Kneschaurek P, Mayr M, eds. *Tumor response monitoring and treatment planning*, 1st ed. Berlin: Springer-Verlag; 1992:219–222.
21. Strauss LG. Application of positron emission tomography in colorectal carcinoma. *Onkologie* 1993;16:232–244.
22. Chaudhuri NK, Murkherjee KL, Heidelberger C. Studies of fluorinated pyrimidines-VII-the degradative pathway. *Biochem Pharmacol* 1959;1:328–341.
23. Wolf W, Presant CA, Servis KL, et al. Tumor trapping of 5-fluorouracil: in vivo ^{19}F NMR spectroscopic pharmacokinetics in tumor-bearing humans and rabbits. *Proc Natl Acad Sci USA* 1990;87:492–496.
24. Shani J, Wolf W. A model for prediction of chemotherapy response to 5-fluorouracil based on the differentiated distribution of 5-^{18}fluorouracil in sensitive versus resistant lymphocytic leukemia in mice. *Cancer Res* 1977;37:2306–2308.
25. Semmler W, Bachert-Baumann P, Gückel F, et al. Real-time follow-up of 5-fluorouracil metabolism in the liver of tumor patients by means of F-19 MR spectroscopy. *Radiology* 1990;174:141–145.
26. Sela S, Husain SR, Pearson JW, et al. Reversal of multidrug resistance in human colon cancer cells expressing the human *MDR1* gene by liposomes in combination with monoclonal antibody or verapamil. *J Natl Cancer Inst* 1995;87:123–128.
27. Wohlhueter RM, McIvor RS, Plagemann PGW. Facilitated transport of uracil and 5-fluorouracil, and permeation of orotic acid into cultured mammalian cells. *J Cell Physiol* 1980;104:309–319.
28. Jacquez JA. Permeability of Ehrlich cells to uracil, thymine and fluorouracil. *Proc Soc Exp Biol Med* 1962;109:132–135.
29. Yamamoto S, Kawasaki T. Active transport of 5-fluorouracil and its energy coupling in Ehrlich ascites tumor cells. *J Biochem* 1981;90:635–642.
30. Domin BA, Mahony WB, Zimmerman TP. Transport of 5-fluorouracil and uracil into human erythrocytes. *Biochem Pharmacol* 1993;46:503–510.

Bone Marrow Uptake of Thallium-201 Before and After Therapy in Multiple Myeloma

Masatoshi Ishibashi, Masaaki Nonoshita, Masafumi Uchida, Kazuyuki Kojima, Naofumi Tomita, Satoko Matsumoto, Ken Tanaka and Naofumi Hayabuchi

Division of Nuclear Medicine, Department of Radiology, Division of Hematology, First Department of Internal Medicine, Kurume University School of Medicine, Kurume City, Japan

We describe a patient with multiple myeloma who was found to have diffuse bone marrow uptake of ^{201}Tl. Magnetic resonance (MR) imaging of the lumbar spine demonstrated abnormal low signal intensity on T1-weighted images and abnormal high signal intensity on T2-weighted images. The bone marrow consisted of 68% plasma cells, and the serum immunoglobulin (Ig)G concentration was 7900 mg/dL. After receiving chemotherapy, the percentage of plasma cells and serum IgG concentration declined and there was a decrease in the bone marrow uptake of ^{201}Tl. However, the MR abnormalities in the lumbar spine showed no change after chemotherapy. This patient illustrates a limitation of the use of MR imaging for evaluation of disease state in patients with multiple myeloma, and demonstrates the potential usefulness of ^{201}Tl imaging in these patients.

Key Words: thallium-201; multiple myeloma; diffuse bone marrow pattern; magnetic resonance imaging; chemotherapy

J Nucl Med 1998; 39:473–475

One of the major goals of imaging in patients with multiple myeloma is to determine changes in disease state after treatment. Waxman et al. (*1*) have described the usefulness of ^{67}Ga imaging to identify a subgroup of multiple myeloma patients with rapidly progressive disease who may benefit from alternative therapy such as irradiation. Recently, the myocardial perfusion agents ^{99m}Tc-sestamibi and ^{99m}Tc-tetrofosmin have been under investigation for nuclear oncology (*2–3*). Magnetic resonance (MR) imaging of the spine has recently been shown

Received Jan. 16, 1997; revision accepted May 6, 1997.

For correspondence or reprints contact: Masatoshi Ishibashi, MD, Division of Nuclear Medicine and Department of Radiology, Kurume University School of Medicine, 67 Asahi-Machi, Kurume City, Fukuoka, 830, Japan.